© 2015. Published by The Company of Biologists Ltd | Journal of Cell Science (2015) 128, 4487-4498 doi:10.1242/jcs.172684

RESEARCH ARTICLE

Spatial and temporal translational control of germ cell mRNAs mediated by the eIF4E isoform IFE-1

Andrew J. Friday[1], Melissa A. Henderson[2], J. Kaitlin Morrison[1], Jenna L. Hoffman[1] and Brett D. Keiper[1,*]

ABSTRACT

Regulated mRNA translation is vital for germ cells to produce new proteins in the spatial and temporal patterns that drive gamete development. Translational control involves the de-repression of stored mRNAs and their recruitment by eukaryotic initiation factors (eIFs) to ribosomes. *C. elegans* expresses five eIF4Es (IFE-1–IFE-5); several have been shown to selectively recruit unique pools of mRNA. Individual IFE knockouts yield unique phenotypes due to inefficient translation of certain mRNAs. Here, we identified mRNAs preferentially translated through the germline-specific eIF4E isoform IFE-1. Differential polysome microarray analysis identified 77 mRNAs recruited by IFE-1. Among the IFE-1-dependent mRNAs are several required for late germ cell differentiation and maturation. Polysome association of *gld-1*, *vab-1*, *vpr-1*, *rab-7* and *rnp-3* mRNAs relies on IFE-1. Live animal imaging showed IFE-1-dependent selectivity in spatial and temporal translation of germline mRNAs. Altered MAPK activation in oocytes suggests dual roles for IFE-1, both promoting and suppressing oocyte maturation at different stages. This single eIF4E isoform exerts positive, selective translational control during germ cell differentiation.

KEY WORDS: mRNA translational control, Oogenesis, *C. elegans*, Translation state array analysis, TSAA, Protein synthesis, Meiotic maturation

INTRODUCTION

Cell fate, proliferation and differentiation are dependent on gene expression, often at the level of protein synthesis (Kimble and Crittenden, 2007). Dysregulation of these processes is associated with human pathologies including infertility, birth defects and cancers (Graff et al., 2008; Song and Lu, 2011). Clinical studies have shown that the eukaryotic translation initiation factor eIF4E is overexpressed in multiple cancers including ovarian, esophageal, breast, thyroid and prostate (Furic et al., 2010; Ko et al., 2009; Kouvaraki et al., 2011; Salehi and Mashayekhi, 2006). Its overexpression upregulates the translation of mRNAs for cell cycle, growth and reactive oxygen species (ROS) regulatory proteins (De Benedetti and Graff, 2004; De Benedetti and Rhoads, 1990; Rosenwald, 2004; Rosenwald et al., 1993), leading to the cancer phenotype. However, eIF4E-1 depletion by just 50% prevents lung cancer growth in mice (Truitt et al., 2015). eIF4E is essential for cap-dependent protein synthesis in order to recruit mRNAs to the ribosome for translation. Specifically, eIF4E binds both the 7-methylguanosine 5′-cap of mRNAs and the scaffolding translation initiation factor eIF4G (Marcotrigiano et al., 1997). eIF4G assembles initiation factors, the 40S ribosomal subunit and mRNA to form the 48S complex, the rate-limiting step for protein synthesis (Gingras et al., 1999; Lamphear et al., 1995; Liu et al., 2003). The selection of cap-dependent mRNAs by eIF4E can alter cell fate by promoting growth and proliferation (De Benedetti and Graff, 2004; De Benedetti and Rhoads, 1990). eIF4E-mediated recruitment of mRNAs can be inhibited by eIF4E-binding proteins (4EBPs), which bind to the dorsal or lateral side of eIF4E to prevent association with eIF4G (Igreja et al., 2014). Cap-dependent recruitment is thereby inhibited, allowing cap-independent initiation to prevail (Contreras et al., 2008; Fukuyo et al., 2011). Growth factor signaling activates mTOR kinase to phosphorylate 4EBP, causing a dissociation from eIF4E and promoting cap-dependent protein synthesis.

Evidence suggests that eIF4E also regulates mRNAs in germ cells. Five isoforms of eIF4E (IFE-1–IFE-5) are expressed in the nematode *C. elegans* (Jankowska-Anyszka et al., 1998; Keiper et al., 2000). We have previously shown that individual isoforms regulate a unique subset of mRNAs in a tissue-specific manner (Amiri et al., 2001; Dinkova et al., 2005; Henderson et al., 2009; Kawasaki et al., 2011; Song et al., 2010). Given that all IFEs bind to mRNA caps, these findings suggest a selective cap-dependent regulation that goes beyond mTOR regulation. For example, although IFE-2 and IFE-4 are expressed in somatic tissue, they regulate different mRNAs whose products drive different developmental events. IFE-2 regulates aging, whereas IFE-4 regulates nerve and muscle tissue function (Dinkova et al., 2005; Syntichaki et al., 2007). IFEs 1, 3 and 5 (and to a lesser extent IFE-2) are expressed in the germ line and are involved in gamete development (Henderson et al., 2009; Keiper et al., 2000; Song et al., 2010). Germ line and embryonic development require essential proteins for cellular differentiation, maturation and viability. During gametogenesis stored mRNAs are utilized when transcription is largely silenced due to chromosomal condensation (Kelly and Fire, 1998; Seydoux et al., 1996). Studies in germ cells from multiple species have shown that available ribosomes translate these mRNAs as they become de-repressed, but recent evidence suggests that translation initiation factors take part in both the repression and subsequent recruitment (Dworkin and Dworkin-Rastl, 1990; Ghosh and Lasko, 2015; Goodwin and Evans, 1997; Macdonald and Smibert, 1996; Mendez and Richter, 2001; Wormington, 1993). In *Xenopus laevis* oocytes, for example, meiotic maturation is arrested by translational suppression of cyclin-B mRNA, which contains a cytoplasmic polyadenylation element (CPE) in the 3′-untranslated region (3′UTR). Repression of cyclin-B mRNA occurs when the eIF4E–maskin–CPEB (CPE-binding factor) complex forms. Maskin acts as a specialized 4EBP bound to mRNA that inhibits recruitment of an initiation complex through eIF4G (Barnard et al., 2005). To induce oocyte maturation,

[1]Department of Biochemistry and Molecular Biology, Brody School of Medicine at East Carolina University, Greenville, NC 27834, USA. [2]Department of Molecular Sciences, DeBusk College of Osteopathic Medicine, Lincoln Memorial University, Harrogate, TN 37752, USA.

*Author for correspondence (keiperb@ecu.edu)

Received 14 April 2015; Accepted 2 November 2015

Journal of Cell Science (2015) 128, 4487-4498 doi:10.1242/jcs.172684

progesterone activates a signaling cascade that results in CPEB phosphorylation, Maskin dissociation from eIF4E and cap-mediated recruitment of the de-repressed mRNA. Translation of these products reinitiates the cell cycle and oocyte maturation (Barnard et al., 2005; Cao and Richter, 2002). Dysregulation of the first meiotic division in human oocytes is a large contributor to infertility and miscarriage (Hunt, 1998). mRNA translational control thus provides a substantive link to oncogenesis and reproductive health.

IFE-1 is a nematode eIF4E isoform bound to the 4EBP-like protein PGL-1 (Amiri et al., 2001). Together these proteins reside in P granules, which are germ-line-specific ribonucleoprotein (mRNP) complexes containing stored mRNAs (Kawasaki et al., 1998). Based on localization in these mRNPs, we hypothesize that IFE-1 uniquely catalyzes the subsequent translation of stored mRNAs during germ cell development. Supporting this hypothesis, *ife-1* mutant worms have substantial developmental defects during gametogenesis and embryogenesis. These include a temperature-sensitive defect in cytokinesis in secondary spermatocytes, which results in a complete lack of mature sperm. Even under sperm-permissive conditions, *ife-1* worms still show a reduced rate of oocyte production, viability and early embryonic lethality (Henderson et al., 2009). We have used a genomic approach called translation state array analysis (TSAA) to identify 77 mRNAs that rely on IFE-1 for positive translational control. Furthermore, IFE-1 carries out spatiotemporal recruitment of mRNAs involved in meiosis, mitogen-activated protein kinase (MAPK) activation, oocyte maturation and embryogenesis.

RESULTS

IFE-1 regulates the translational efficiency of a distinct population of mRNAs

Our previous studies have shown that IFE-1 is required for the efficient translation of several developmentally controlled mRNAs in the *C. elegans* germ line (*pos-1*, *oma-1*, *mex-1*, *pal-1* and *glp-1*) (Henderson et al., 2009). Here, we determined the entire population of messages that are IFE-1-dependent using TSAA (Chappell et al., 2013; Dinkova et al., 2005; Song et al., 2010). Using Affymetrix microarrays, we quantified the partitioning of every mRNA into ribosome-bound and unbound pools (Fig. 1A). We derived a

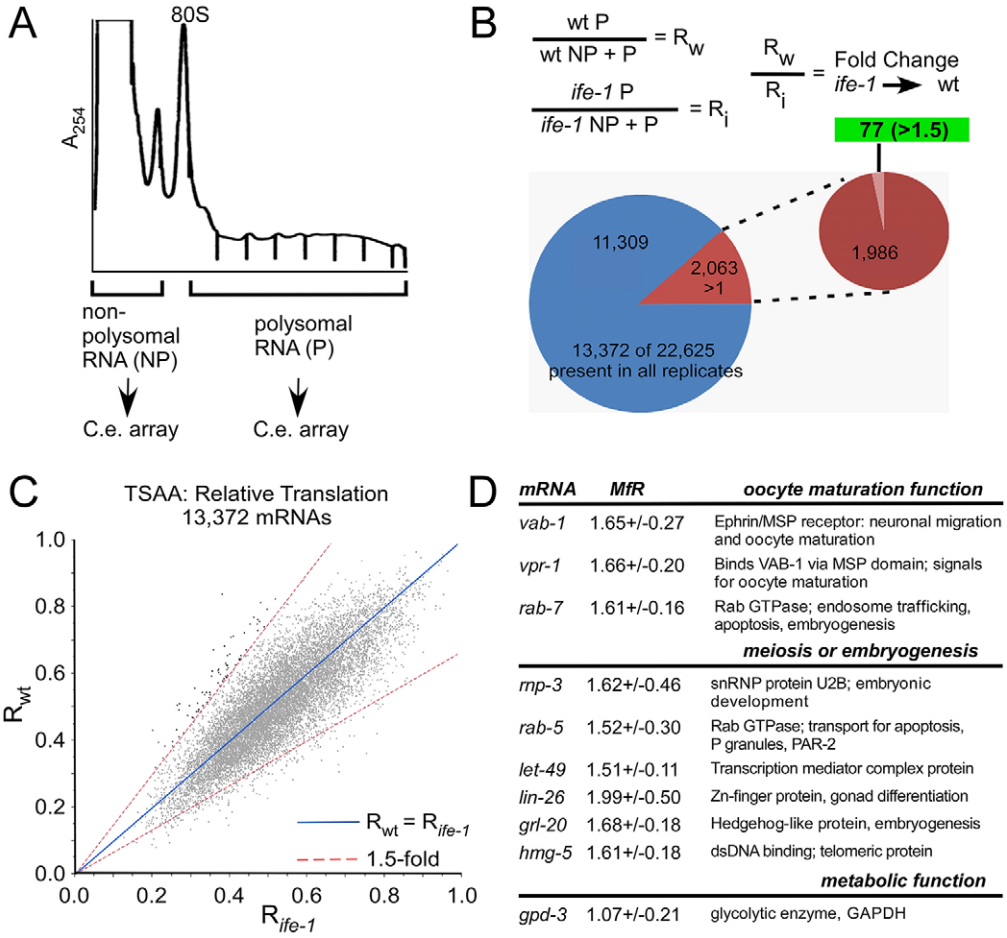

mRNA	MfR	oocyte maturation function
vab-1	1.65+/-0.27	Ephrin/MSP receptor: neuronal migration and oocyte maturation
vpr-1	1.66+/-0.20	Binds VAB-1 via MSP domain; signals for oocyte maturation
rab-7	1.61+/-0.16	Rab GTPase; endosome trafficking, apoptosis, embryogenesis
		meiosis or embryogenesis
rnp-3	1.62+/-0.46	snRNP protein U2B; embryonic development
rab-5	1.52+/-0.30	Rab GTPase; transport for apoptosis, P granules, PAR-2
let-49	1.51+/-0.11	Transcription mediator complex protein
lin-26	1.99+/-0.50	Zn-finger protein, gonad differentiation
grl-20	1.68+/-0.18	Hedgehog-like protein, embryogenesis
hmg-5	1.61+/-0.18	dsDNA binding; telomeric protein
		metabolic function
gpd-3	1.07+/-0.21	glycolytic enzyme, GAPDH

Fig. 1. Translational State Array Analysis (TSAA) identified mRNAs translationally regulated by IFE-1. (A) Polysome profile of whole worm lysates resolved on a 10–45% sucrose gradient. Absorbance was continuously monitored at 254 nm during fractionation. RNA derived from non-polysomal (NP) fractions (1–4) and polysomal (P) fractions (6–11) were pooled separately for the TSAA. (B) The mean fold change of relative polysomal probe signal (MFR) was calculated using customized Excel data sheets with formulas created by the authors. MFR values were sorted and culled from the initial 22,629 probe output signals to a list of 77 mRNAs with an MFR>1.5 and an MFR–s.d.>1.0. Known IFE-1-dependent mRNA *oma-1* (Henderson et al., 2009) was not detected in the TSAA. mRNAs *pos-1*, *pal-1*, *mex-1* and *glp-1* had MFR<1.5; however changes in abundance (e.g. *pos-1*, Fig. S3B and S4) or less sensitive detection in the polysome fractions might have reduced the statistical relevance of such changes. Interestingly, 209 mRNAs showed a >1.5-fold increase in the absence of IFE-1. These were not further characterized in this study. (C) Bivariate response of mean R_w versus mean R_i for the 13,372 mRNAs statistically 'present' in all three biological replicates, derived in JMP Pro10 software. (D) Representative mRNAs of known germ line or embryonic regulatory function and their calculated MFR values.

Journal of Cell Science (2015) 128, 4487-4498 doi:10.1242/jcs.172684

measure of the relative change (R value) in polysome loading between wild-type and *ife-1* strains (Fig. 1B). This method directly assessed the translational efficiency of each mRNA, independent of changes in the abundance, by quantifying both the polysomal (P) and non-polysomal (NP) content of mRNAs, rather than just the amount in polysomes. Calculating a mean fold change in R-value (MFR) allowed us to prioritize mRNAs with markedly altered translational efficiency. From the arrays, we also derived the mean fold polysomal loading change (MFP), as well as the change in total mRNA (MFT) from sums of the NP and P signals, for wild-type and *ife-1* worms. The mRNA subset with the largest change in total signal (MFT) substantially overlapped with the subset of mRNAs with the largest change in polysome signal (MFP; Fig. S1B). By contrast, the relative translational efficiency group (MFR) shares just eight mRNAs with the polysome MFP group. Therefore, measuring only polysomal mRNA content would be a misleading assessment of translational control.

A prioritized list of 77 IFE-1-dependent mRNAs was derived from the 13,372 mRNAs reliably detected and statistically relevant in all three biological replicates. Each mRNA showed greater than 1.5-fold increase in relative polysome loading (MFR) when IFE-1 was present (Fig. 1B,C), which was largely maintained in the individual replicates (Fig. S2). Of the 77 candidates, 25 had known phenotypes or functions. Among these, only nine were relevant to the germ line or early embryogenesis (Fig. 1D), and these were pursued. Several (*vab-1*, *vpr-1* and *rab-7*) encode genes that regulate MAPKs (likely MPK-1) in late stage oocyte maturation (Fig. 1D; Fig. S3A). Others (*lin-26*, *rab-5*, *rnp-3*, *let-49*, *hmg-5* and *grl-20*) are essential for meiotic progression or embryonic development. The identification of these mRNAs is consistent with previous biochemical characterizations of the role of IFE-1 in protein synthesis, specifically in oocytes and early embryos, as well as the *ife-1*(*bn127*) phenotype (Amiri et al., 2001; Henderson et al., 2009). In contrast to the IFE-1-dependent mRNAs, most other mRNAs showed no change, as evidenced by their position along the R_{wt}=$R_{ife\text{-}1}$ diagonal. Their translational efficiency was unchanged in the *ife-1*(*bn127*) mutant worms (Fig. 1C; Fig. S3A). Many IFE-1-independent messages were housekeeping mRNAs (e.g. actin, tubulin and GAPDH), although some were cell cycle and kinase mRNAs (*mpk-1* and *cdk-4*), and cell fate mRNAs (e.g. *pgl-1*; Fig. S3A). Remarkably, sperm-specific mRNAs, such as those encoding the 28 known major sperm proteins (MSPs) were unchanged in relative R value in the TSAA. Spermatogenesis is compromised in the *ife-1* mutant even at the permissive temperature used in the TSAA (Henderson et al., 2009). MSPs have been shown by proteomic analysis to be deficient in *ife-1* worms (Kawasaki et al., 2011). By segregating the MFR and MFT for all identified *msp* mRNAs, our data showed them to be underrepresented in the total population but unchanged in their translational efficiency (Fig. S3C,D). Decreased MSP protein in worms lacking IFE-1 is therefore due to lack of mRNA rather than translational control.

IFE-1 recruits mRNAs that regulate germ cell differentiation and maturation events

In order to determine the detailed translational efficiency of mRNAs, we analyzed the polyribosomal loading of mRNAs by sucrose gradient centrifugation. Based on known *ife-1* mutant phenotypes, we focused on known mRNAs that regulate germ cell fates during meiosis and oocyte maturation. Polysome profiles of wild-type and *ife-1* lysates that resolve mRNAs by incremental ribosome loading were recorded and fractionated (Fig. 2A,B). mRNAs at the top of the gradient, above the 80S peak, do not have ribosomes bound and are not translating. This includes mRNAs in mRNP structures such as P granules. A constitutive P granule protein, PGL-1, remained at the top of the gradient in non-sedimenting complexes (Fig. 2C,D), indicating that P-granule-bound mRNAs do not co-sediment with ribosome-bound mRNAs. mRNAs that sediment past the 80S peak have multiple ribosomes bound. These sediment progressively further with greater translational efficiency. Ribosome loading increases exponentially rather than linearly along the gradient. mRNAs that shift from 'light polysomes' (fractions 5–7) to 'heavy polysomes' (fractions 8–10) in the gradient have undergone a greater change in protein synthesis efficiency than a similar shift near the top or middle of the gradient. Only a modest decrease in the total polysome content was observed for *ife-1*. This is to be expected because global protein synthesis (even cap-dependent) is still being supported through the other eIF4E isoforms present.

mRNAs with potential roles in the oocyte maturation defect – *vab-1*, *vpr-1*, *rab-7* and *rnp-3*

The results of the TSAA led us to address the translation efficiency of germline mRNAs that contribute to the phenotype observed in the *ife-1* mutant. TSAA results led us to discover new IFE-dependent mRNAs *vab-1*, *vpr-1*, *rab-7* and *rnp-3*, translationally controlled in late oocytes. To determine changes in the translational efficiency of mRNAs identified in our TSAA (MFR>1.5), RNA from each sucrose fraction was subjected to real-time PCR (qPCR). Primers were used to detect *vab-1* (MSP receptor), *vpr-1* (MSP-like protein) and *rab-7* (Rab GTPase) mRNAs. VAB-1 suppresses the MAPK activity required for late stage oocyte maturation. In the *ife-1* worms, there was a reduction in heavy polysomal *vab-1* mRNA (fractions 8–10) with a corresponding increase in non-translating and light polysomal *vab-1* mRNA (fractions 3–5; Fig. 2E). This decrease in translational efficiency indicates that *vab-1* utilizes primarily IFE-1 for initiation. mRNAs encoding VPR-1 and RAB-7 also showed a marked decrease in heavy polysome loading, with a corresponding increase in non-translating mRNA (Fig. 2F,G). More non-translating *vpr-1* and *rab-7* mRNA indicated that initiation events were less frequent in the absence of IFE-1. The decrease in translational efficiency of *vpr-1* and *rab-7* indicates that, in addition to *vab-1*, two mRNAs involved in VAB-1 signaling are also translationally recruited by IFE-1. Another mRNA strongly regulated by IFE-1 encoded RNP-3, a small nuclear ribonucleoprotein (snRNP) that was identified in the TSAA. Loss of RNP-3 activity has been shown to cause embryonic lethality (Saldi et al., 2007). Like *vab-1*, *vpr-1* and *rab-7* mRNAs, *rnp-3* translation was much less efficient in the absence of IFE-1, confirming the 1.6-fold decrease observed in the TSAA (Fig. 2L). Much of its mRNA shifted from heavy polysomes and monosomes into the non-translating region of the gradient (fractions 1–3; Fig. 2H). General mRNA translation was not perturbed, as evidenced by the distribution of the housekeeping *gpd-3* (GAPDH) mRNA (Fig. 2I). Therefore, other eIF4E isoforms support translation initiation of this mRNA and many others (e.g. *nos-3*, profile not shown; see Fig. 1C). These data show that proteins (VAB-1, VPR-1 and RAB-7) that regulate oocyte MAPK are strongly dependent on IFE-1 for their synthesis. The biological consequences of their translational control will be addressed later in this study.

mRNAs that shift in polysome distribution – *ran-1* and *gld-1*

Other mRNAs appear to be regulated only in part by IFE-1. RAN-1, similar to RAB-7, is a GTPase that regulates VAB-1 trafficking in

Journal of Cell Science (2015) 128, 4487-4498 doi:10.1242/jcs.172684

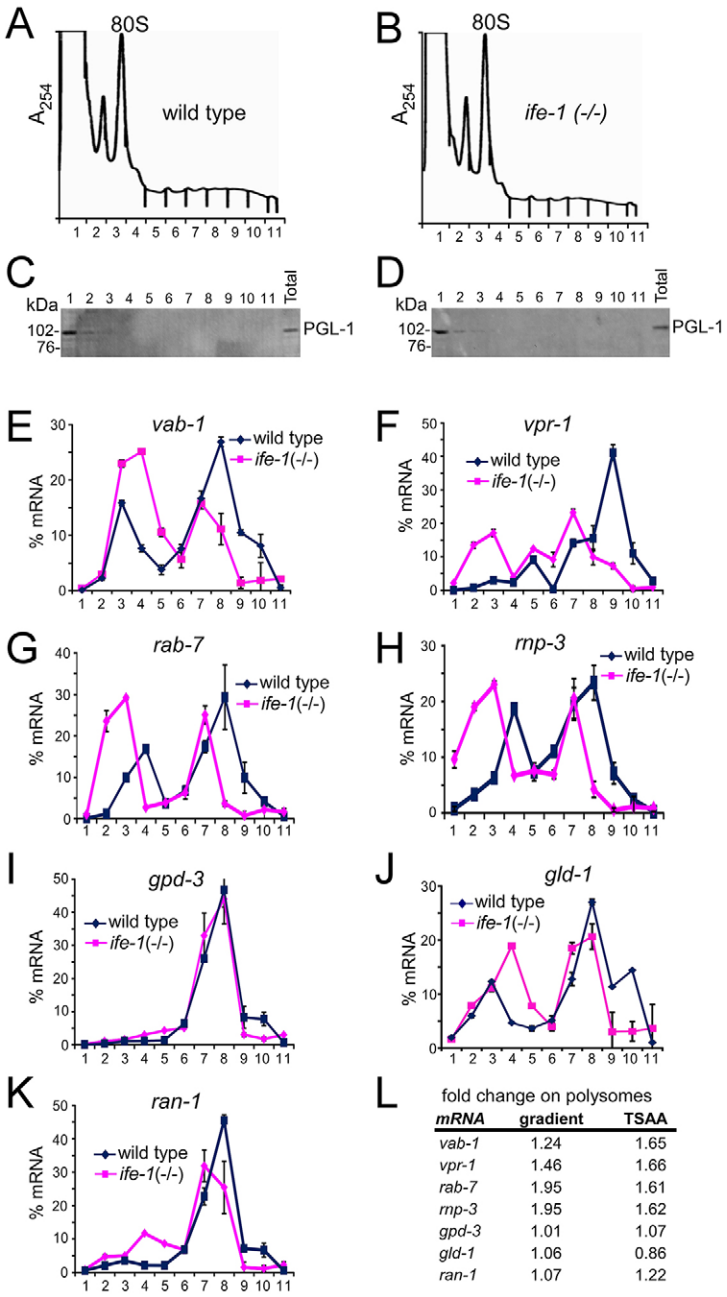

mRNA	gradient	TSAA
vab-1	1.24	1.65
vpr-1	1.46	1.66
rab-7	1.95	1.61
rnp-3	1.95	1.62
gpd-3	1.01	1.07
gld-1	1.06	0.86
ran-1	1.07	1.22

Fig. 2. Polysome fractionation analysis of germ line mRNAs. Polysome profiles for wild-type (A) and *ife-1*-null (B) whole worm lysates resolved on a 10–45% sucrose gradient. Profiles were derived as in Fig. 1 and represent one of three biological replicates. Resolution is such that individual polysomes were apparent to at least the 6-mer size, and the monosome (80S) peak absorbance is the largest. The sedimentation of P granules was determined in identical gradients by western blot for PGL-1 of each fraction and the input lysates (C and D), indicating that P granules remain at the top of the gradient. The quantitative distribution of individual mRNAs were assayed throughout the gradients (E–K). mRNA encoding *vab-1* (E), *vpr-1* (F), *rab-7* (G), *rnp-3* (H), *gpd-3* (I), *gld-1* (J) and *ran-1* (K), was quantified by qPCR to indicate changes in translational efficiency. mRNA signal was normalized to total RNA content in each fraction. Results are mean±s.d. relative qPCR values (n=3) for each fraction, relative to the sum of all fractions. (L) A table compares polysome-loading changes as quantified by qPCR across gradients versus values from the TSAA. TSAA MFR values with s.d. were: *vab-1*=1.65±0.27, *vpr-1*=1.66±0.20, *rnp-3*=1.07±0.03, *gpd-3*=1.07±0.21; *gld-1*=0.86±0.15, *rab-7*=1.61±0.16, *ran-1*=1.22±0.08. The s.d. from qPCR is not comparable to the triplicate s.d. as determined by TSAA, so no comparison is shown. Exact UV profiles and mRNA positions vary relative to previous determinations (e.g. Henderson et al., 2009) because of small differences in gradient composition, sedimentation time or sample amount. All gradient comparisons used paired samples in the same centrifugation.

maturing oocytes. The dependence of *ran-1* mRNA on IFE-1, measured by TSAA, was considerably lower (Fig. 2L). However, when assessing the translational efficiency by resolved polysome gradients, a more complex distribution of *ran-1* mRNA was evident. In the absence of IFE-1, *ran-1* showed a modest decrease in heavy polysome loading. Most of its redistribution was among polysomes of smaller sizes (fractions 4–7; Fig. 2K), rather than out of polysomes altogether. Given that all polysomes were pooled for the TSAA, such changes in *ran-1* translation would not have been reflected in the MFR. This points out the limitation of assessing simple 'on–off' state translation assays, and suggests that the TSAA underestimates the translational impact for some mRNAs and overestimates for others. Quantifications by both means, however, are generally consistent (Fig. 2L), and substantiate the use of TSAA to screen for some (but not all) IFE-1-regulated mRNAs. A complex polysome profile is also found for *gld-1* mRNA, which encodes a crucial protein in germ cell development. GLD-1 is an mRNA-binding protein that suppresses mitosis and promotes meiosis by repressing the translation of key regulatory mRNAs, like *glp-1* (Hansen et al., 2004b; Jones et al., 1996). The translational efficiency of *gld-1* mRNA in *ife-1* worms was diminished as indicated by a shift in the distribution of its mRNA, but it was not lost from polysomes altogether. The most efficiently translating *gld-1* (heavy polysomes, fractions 9–10) was lost, and a strong peak in fractions 4–5 (light polysomes) appeared (Fig. 2J). The redistribution of just one peak suggests that IFE-1 recruits a limited subset of *ran-1* and *gld-1* mRNAs. Such a complex redistribution could indicate that other IFE isoforms weakly initiate their translation in all tissues. More likely, however, is that IFE-1 strongly recruits *gld-1* and *ran-1* mRNAs in particular regions of the germ line, whereas other IFEs initiate their translation elsewhere.

Journal of Cell Science (2015) 128, 4487-4498 doi:10.1242/jcs.172684

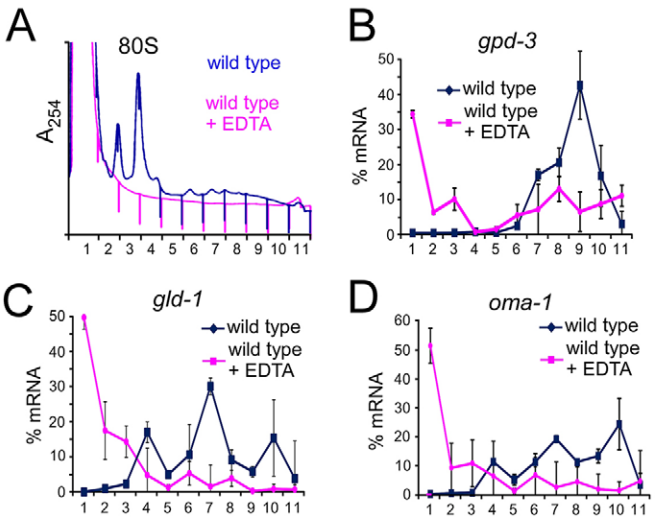

Fig. 3. Release of regulated and non-regulated mRNAs from polysomes by magnesium chelation. Gradient UV profiles for untreated (blue) or EDTA-treated (pink) lysates from wild-type worms were overlaid to show disruption of ribosome association and loss of polysomes (A). The quantitative distribution of individual mRNAs encoding *gpd-3* (B), *gld-1* (C), and *oma-1* (D), quantified by qPCR, are shown. Results are mean±s.d. relative qPCR values (n=3) for each fraction, relative to the sum of all fractions. The bulk of all mRNAs were displaced to the top of the gradient. 'Release' of mRNAs from lower fractions demonstrated that sedimentation was due to association with ribosomes, rather than dense mRNPs, which do not require Mg^{2+}. As in Fig. 2, the mRNA signal was normalized to the total RNA content in each fraction.

Several of the IFE-1-dependent mRNAs have also been found in mRNP structures (e.g. *gld-1* and *oma-1*) (Detwiler et al., 2001; Jeong et al., 2011; Schisa et al., 2001), and it is possible that their sedimentation far into the gradient could be due to non-translating complexes. To test this, we added EDTA to lysates to chelate Mg^{2+} and separate all ribosomal complexes prior to centrifugation (Fig. 3A). mRNP binding does not require Mg^{2+}, so bound mRNAs sediment as before. However, we found that all mRNAs tested, whether they were regulated by IFE-1 (Fig. 3C,D) or not (Fig. 3B), were displaced to the top of the gradient in the absence of Mg^{2+}. Release demonstrated that their sedimentation was due to bound ribosomes rather than a dense bound mRNP complex.

IFE-1 mediates spatial and temporal translational control throughout the gonad

Many germline mRNAs in *C. elegans* are regulated by repression through proteins binding to their 3′UTRs. These mRNAs need to be activated to bind ribosomes. We hypothesize that as such proteins release the 3′UTRs, IFE-1 plays an active role in recruiting these mRNAs for translation initiation in a spatiotemporal manner. To determine the ability of IFE-1 to recruit de-repressed mRNAs in the proper time and place, we used an *in situ* 3′UTR reporter assay. We visually monitored the translation of GFP-fused transgene mRNAs to observe changes in protein expression when IFE-1 was depleted by RNA interference (RNAi). As the reporter 3′UTR becomes de-repressed, GFP should be expressed in appropriate germ cells. If regulation of these mRNAs is mediated solely by de-repression, GFP expression will be unaffected by the loss of any one eIF4E isoform. However, if only IFE-1 is able to recruit these mRNAs as they become de-repressed, GFP expression from these mRNAs will not occur. This assay provides the advantage of being able to monitor translational control of an mRNA within single cells as they progress through the germ line in live worms.

Translation of *gld-1* mRNA in distal oocytes

GLD-1 is expressed in immature oocytes in the distal end of the gonad where it promotes meiosis, and its expression is translationally controlled by the 3′UTR (Francis et al., 1995; Hansen et al., 2004b). Having established that *gld-1* mRNA was regulated by IFE-1 in the polysome analysis (Fig. 2J), we then determined that GLD-1 expression was regionally dependent on IFE-1 for its translation. Using an *in vivo* reporter assay with an N-terminal fusion of GFP to the *gld-1* open reading frame (ORF), and the *gld-1* 3′UTR, fluorescence microscopy showed that *gld-1–gfp* mRNA became de-repressed in immature oocytes in syncytium (Fig. 4A). Upon depletion of IFE-1 by RNAi, the fluorescence in the whole distal region of the gonad was visibly diminished. Quantifying the mean GFP fluorescence intensity per exposure time (Fl/t), there was a reproducible twofold increase in GLD-1–GFP expression when IFE-1 was present (Fig. 4B). Our data show that in immature oocytes, IFE-1 uniquely promotes the translation of *gld-1* mRNA.

Spatial and temporal translation of *pos-1*, *tbb-2* and *pgl-1* mRNAs

For subsequent assays, we tested reporter constructs that fuse GFP to histone H2B and bear the 3′UTRs of various mRNAs, so that the fluorescence becomes localized in the oocyte nuclei. We previously demonstrated that *pos-1* mRNA requires IFE-1 for translation (Henderson et al., 2009). *pos-1* (posterior segregation) is natively repressed throughout most of oogenesis. It is de-repressed only in late stage oocytes, so newly synthesized POS-1 protein can help to establish early embryonic polarity. The *pos-1* 3′UTR reporter showed accumulation of the H2B–GFP product only in nuclei of the three largest oocytes of live worms. Following IFE-1 knockdown, H2B–GFP expression was nearly absent from oocytes of all stages (Fig. 4C). Quantification of GFP (Fl/t) showed a threefold increase in *pos-1* 3′UTR reporter translation by IFE-1 (Fig. 4D). This indicates that when the *pos-1* mRNA became natively de-repressed in the −3, −2 and −1 oocytes, it was primarily IFE-1 that recruited the mRNA for translation. We also tested a *tbb-2* 3′UTR reporter. *tbb-2* encodes β-tubulin and is expressed at high levels in the *C. elegans* germ line (Lu et al., 2004). Upon IFE-1 depletion there was no visible decrease in H2B–GFP expression from the *tbb-2* 3′UTR (Fig. 4E). Comparison of GFP (Fl/t) in the late stage oocytes (−3, −2 and −1 oocytes) showed no significant change (Fig. 4F). This was expected because *tbb-2* is not a translationally repressed mRNA in germ cells (Merritt et al., 2008) and its translation is not dependent on IFE-1. Other germ cell IFEs can recruit β-tubulin mRNA (and presumably all de-repressed mRNAs) with equal efficiency. Thus, the observed temporally regulated mRNA translation is specific to IFE-1 and not the result of suppressed general cap-dependent initiation.

PGL-1 is an RNA-binding protein that localizes IFE-1 protein to P granules. An H2B–GFP reporter with *pgl-1* 3′UTR was fully active for translation in early meiotic germ cells (distal) from control RNAi-treated worms, and remained modestly abundant in late stage oocytes. Interestingly, when IFE-1 was depleted, GFP from *pgl-1* 3′UTR mRNA continued to be expressed in early germ cells and appeared to increase in all of the later stage oocytes (Fig. 4G). Quantification showed a more than twofold increase in GFP in the −3, −2 and −1 oocytes (Fig. 4H). Increased mRNA translation in the absence of IFE-1 suggests that other IFE isoforms more efficiently recruit *pgl-1* mRNA. The effect might be due to *pgl-1* mRNA stabilization, given that the levels of *pgl-1* were elevated in *ife-1* worms (Fig. S3B), but its translational efficiency was unchanged (Fig. S3A). By depleting IFE-1 *in vivo* from these

Journal of Cell Science (2015) 128, 4487-4498 doi:10.1242/jcs.172684

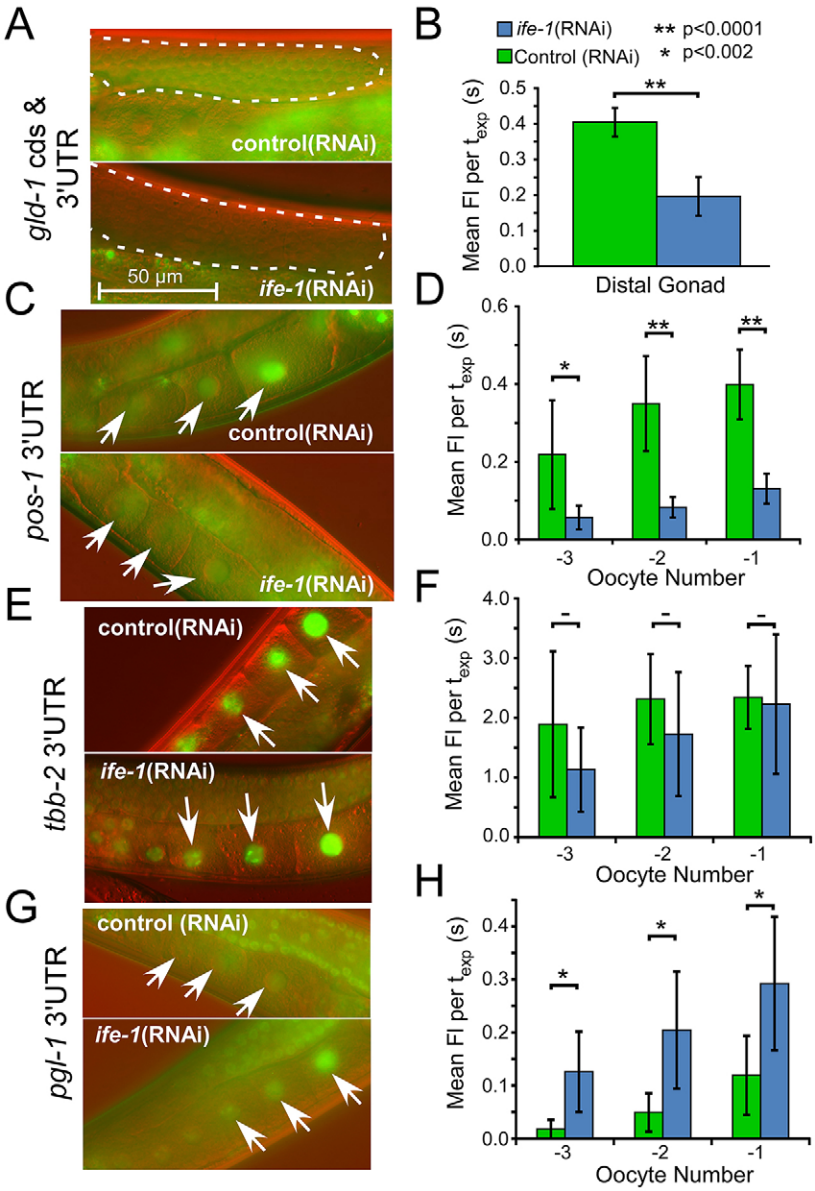

Fig. 4. IFE-1 regulates mRNAs in a spatiotemporal manner in the germ line. Microscopy of *in vivo* reporter constructs translationally regulated by 3′UTRs for *gld-1* (A), *pos-1* (C), *tbb-2* (E) and *pgl-1* (G). In the absence of IFE-1, de-repressed reporters under IFE-1 translational regulation were not efficiently expressed (B,D). Quantification of fluorescence was utilized from minimally five exposures, and mean fluorescence normalized to exposure time (FI/t) was linear. This fluorescence measure showed that the *tbb-2* 3′UTR (F) reporter construct had no significant change in GFP expression (n=10). The *pos-1* 3′UTR (D) (n=11) and *gld-1* 3′UTR (B) (n=12) reporter constructs had a significant decrease in GFP expression, whereas *pgl-1* (H) exhibited a significant increase in GFP expression in the absence of IFE-1 (n=11). Results are mean fluorescence arbitrary units per exposure time ±s.d. ($n\geq5$). *P<0.002; **P<0.0001; –, indicates no significant difference (two tailed t-test).

transgenic GFP reporter strains, we identified a unique role of IFE-1 in positive translational control of certain mRNAs within individual germ cells at critical junctures during development. Furthermore, IFE-1 regulates these mRNAs in conjunction with their 3′UTR sequences and therefore must coordinate with the proteins mediating their repression.

IFE-1 regulates MAPK activation in maturing oocytes

Without IFE-1, oocytes grow slowly and mature inefficiently (Henderson et al., 2009). In *C. elegans*, growing oocytes naturally arrest in meiotic prophase before maturation and fertilization (McCarter et al., 1999). Meiotic arrest is due to signaling from VAB-1, which suppresses MAPK (Cheng et al., 2008; Miller et al., 2003). VAB-1 is the Ephrin receptor tyrosine kinase expressed both in germ cells and their somatic neighbors. MSPs released from sperm cause VAB-1 to be relocalized and degraded (Cheng et al., 2008). VAB-1 degradation restores MAPK activation, induces cyclin-B synthesis and causes resumption of the cell cycle (Miller et al., 2003). Phosphorylated MAPK is a marker of cell cycle progression and maturation. Wild-type gonads display activated MAPK only in the maturing (−1) oocyte when immunostained for diphosphorylated (diphospho)-MAPK (Fig. 5A). In worms depleted of IFE-1 by RNAi, gonads were devoid of activated MAPK (Fig. 5C). By contrast, *vab-1* animals showed no suppression of MAPK from the −1 through to the −5 fully grown oocytes (Fig. 5B). As previously published, removing the suppressive role of VAB-1 permits a precocious oocyte maturation phenotype (Miller et al., 2003). When IFE-1 was knocked down in worms devoid of VAB-1, we observed even broader MAPK activation, earlier than the −5 oocyte, back to pachytene stages (Fig. 5D). This indicates that IFE-1 suppresses MAPK activity independently of VAB-1 in very early oocytes. In the absence of both IFE-1 and VAB-1, MAPK activation in all the later stage oocytes (−1 through to −5) was diminished relative to the −1 oocyte in gonads with IFE-1 (Fig. 5A), but greater than those lacking only IFE-1 (Fig. 5C). This indicates that IFE-1 suppresses MAPK activation in immature oocytes (both VAB-1-dependent and independent), while still promoting MAPK activation in the late stage (−1) oocyte. Alternating suppression and activation of MAPK likely involves recruitment of several mRNAs in the immature

Journal of Cell Science (2015) 128, 4487-4498 doi:10.1242/jcs.172684

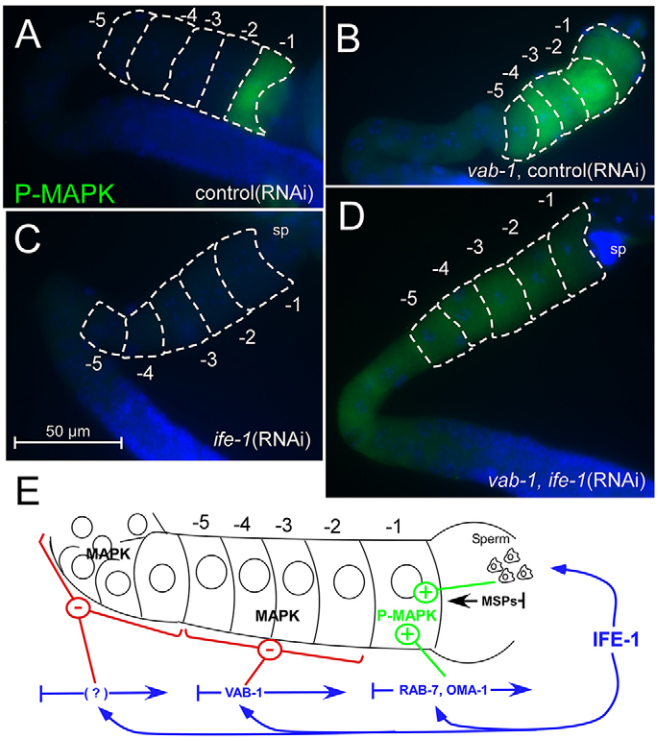

Fig. 5. Analysis of MAPK activation in early and late stage oocytes. Wild-type (A) and *vab-1*-null (B) dissected worm gonads were fixed and immunostained for activated di-phospho-MAPK (P-MAPK) after treatment with control RNAi. Similarly, *ife-1* RNAi knockdown in wild-type (C) and *vab-1*-null (D) worms exhibited a loss of MAPK activation in the −1 oocyte (C) and precocious low levels of MAPK activation in *vab-1*-null *ife-1*(RNAi) oocytes (D). (E) Proposed model for IFE-1 regulation of late oocyte proteins and MAPK regulation in maturing oocytes.

versus the maturing oocytes. Given that IFE-1 is expressed throughout all germ cell stages (Amiri et al., 2001), we suggest that IFE-1 exerts multiple phases of mRNA recruitment along the path of oogenesis (Fig. 5E).

The contribution of sperm versus cell-autonomous signals for maturation competence becomes important as oocytes become fully grown. Given that *ife-1*(*bn127*) worms do not make viable sperm at 25°C (Henderson et al., 2009), we sought to determine which signal is compromised. However, the loss of sperm was not observed in the *ife-1*(RNAi) phenotype (25°C; Fig. 5C). To rule out that loss of MAPK activation in the −1 oocyte was due to insufficient or crippled sperm, we visualized MAPK under conditions in which wild-type (viable) sperm could substitute for mutant sperm. *vab-1* worms crossed with wild-type males (Fig. 6A) exhibited the same extent of MAPK activation out to the −5 oocyte as uncrossed *vab-1* worms (Fig. 5B). The same immunostaining pattern suggested that the sperm present in the *vab-1* mutant alone are sufficient to promote MAPK activation. We then depleted IFE-1 from *vab-1* worms crossed with wild-type sperm. Again MAPK was activated beyond the −5 position (Fig. 6B), as exhibited by the *vab-1 ife-1* (RNAi) gonads (Fig. 5D). The lack of both VAB-1 and IFE-1 permits this broad, suboptimal MAPK activity throughout the whole proximal gonad.

To address whether sperm–oocyte signaling is altered when IFE-1 is completely absent, we also examined MAPK activation in gonads of *ife-1* worms raised at 15°C (permissive for viable sperm) and 25°C (no sperm). Loss of IFE-1 prevented MAPK activation in both the presence and absence of isogenic sperm (Fig. 6C,D). However, this could be due to lower number of sperm (Henderson et al., 2009) or the under representation of *msp* mRNAs in *ife-1* sperm (Fig. S3D). When wild-type sperm were mated to *ife-1* worms at 15°C and 25°C, we observed a substantial ectopic MAPK activation in post-pachytene oocytes (Fig. 6I,J). This suggests that IFE-1-mediated suppression antagonizes the MAPK activation in early oocytes mediated by potent sperm. We compared MAPK activation changes due to IFE-1 deficiency with an established sperm-deficient mutant. The *fem-2*(*b245*) strain also fails to make viable sperm at 25°C. FEM-2 is a putative protein phosphatase that is known to function in the sperm–oocyte switch (Hodgkin, 1986), but it is unclear what role it plays in post-pachytene oocyte maturation. We have previously shown that unlike *ife-1*, which slows oocyte growth and fertility, *fem-2* has no demonstrable effect on oocyte production or fertility (Henderson et al., 2009). Both *ife-1* and *fem-2* fail to activate MAPK in the mature (−1) oocyte when no sperm was present (Fig. 6D,F). However, unlike *ife-1*, *fem-2* oocytes were competent for MAPK activation at the permissive temperature (Fig. 6E), indicating a potential difference in their sperm or the oocyte response to sperm. When exposed to wild-type sperm, both *ife-1* 'females' and *fem-2* 'females' elicited a broad but dampened MAPK activation (Fig. 6G–J) reminiscent of unregulated MAPK in worms lacking both VAB-1 and IFE-1 (Fig. 5D). These observations suggest that *fem-2* acts downstream of or in parallel to *ife-1* in the pathway to maturation. The simplest interpretation would be that *fem-2* mRNA is likewise IFE-1-dependent; however, we have no evidence for such translational control (TSAA data showed *fem-2* had an MFR of 0.99±0.25). Our findings support a model in which IFE-1-dependent mRNAs promote MAPK activation in the mature (−1) oocyte as well as suppress MAPK activation in immature oocytes (Fig. 7).

DISCUSSION

During germline development, proliferation and differentiation of the stem cells into competent eggs and sperm are regulated by mRNA translational control. Selective protein synthesis of germ cell determinants is governed temporally and spatially by both sequence-specific mRNA repression and translational activation. Much has been described about mRNA repression by RNA-binding proteins (e.g. GLD-1, FBFs, OMA-1, CPEB, Nanos and Pumilio) and how they are vital for germ cell development (reviewed in Friday and Keiper, 2015; Lee et al., 2015; Mendez and Richter, 2001; Nousch and Eckmann, 2013; Parisi and Lin, 2000). Repression, however, represents only the first half of the regulation. Our studies focus on positive translational control of mRNAs and the subsequent developmental activities. Distinct isoforms of translation initiation factor eIF4E carry out selective translational recruitment of mRNAs (Amiri et al., 2001; Dinkova et al., 2005; Henderson et al., 2009; Keiper et al., 2000; Miyoshi et al., 2002; Song et al., 2010). Here, we identified the entire complement of mRNAs recruited by the eIF4E isoform IFE-1 in germ cells. Our data implicate IFE-1-dependent positive translational control in several temporal phases of sperm and oocyte progression, including entry into meiosis and maturation (Fig. 7).

IFE-1 recruits a unique set of mRNAs, distinct from the four other eIF4E isoforms (IFE-2–IFE-5) expressed in *C. elegans*. The deletion of *ife-1* is neither sufficient to substantially disrupt overall protein synthesis, nor the mRNA cap-dependent recruitment step. Three different eIF4E isoforms, IFE-1, -3 and -5, are enriched in the germ line (Keiper et al., 2000). Most individual *ife* strains are viable and display disparate phenotypes.

Journal of Cell Science (2015) 128, 4487-4498 doi:10.1242/jcs.172684

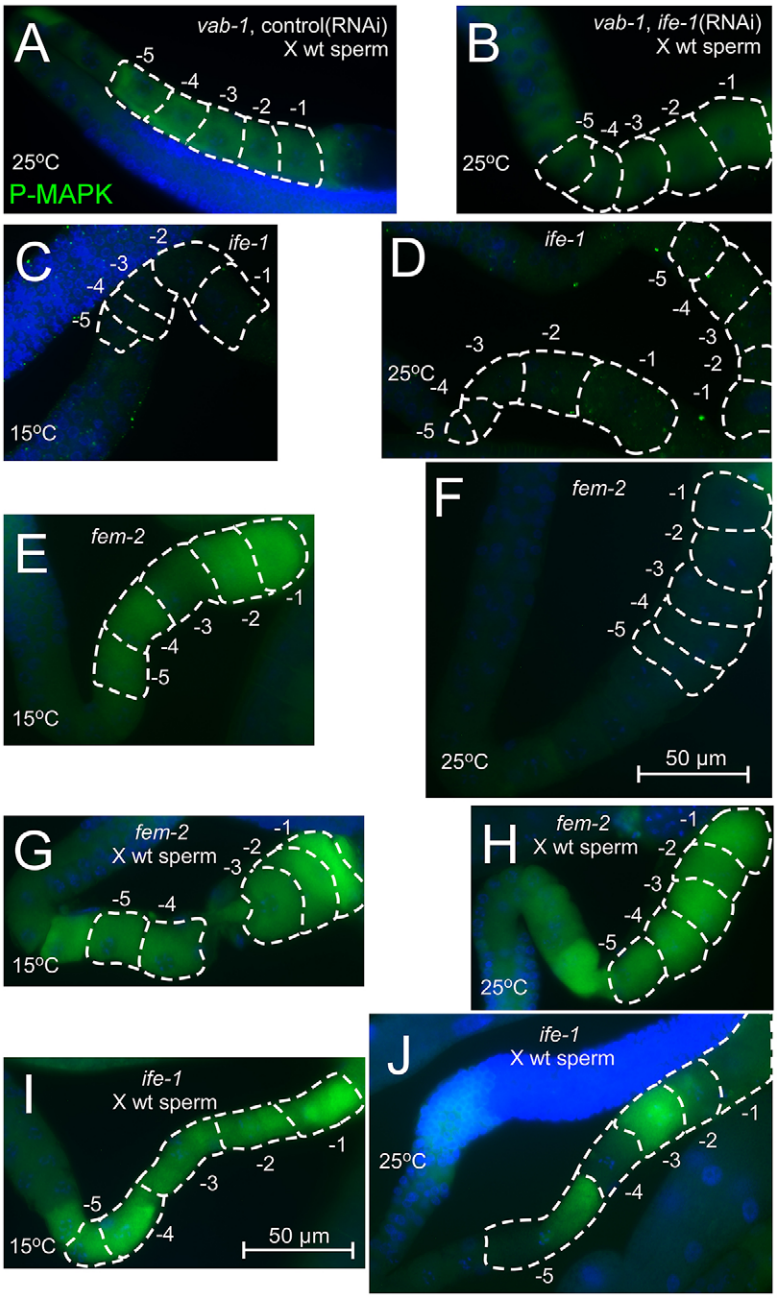

Fig. 6. Analysis of MAPK activation in the presence of wild-type sperm. *vab-1*-null worms treated with control (A) and *ife-1* (B) RNAi were crossed with wild-type (wt) males. Dissected gonads were fixed and immunostained for activated di-phospho-MAPK (P-MAPK). Each germ line exhibited moderate MAPK activation profiles similar to that of uncrossed *vab-1*-null mutants (Fig. 5B,D). *ife-1* worms were grown at the sperm-permissive temperature of (C) 15°C and at the sperm-restrictive temperature of (D) 25°C (no sperm). These gonads displayed a complete loss of MAPK activation as seen in wild-type *ife-1*-knockdown worms (Fig. 5C). *fem-2* worms grown at the sperm-permissive temperature exhibited MAPK activation in the −1 through to −5 oocytes (E), which was lost in feminized gonads without sperm (F). *fem-2* mutants crossed with wild-type sperm had activated MAPK in the −1 through to −5 oocytes (G) that was maintained when feminized (H). *ife-1* worms grown at 15°C (I) and 25°C (J) and crossed with wild-type sperm restored modest MAPK activation that was lost in the *ife-1*-null and -knockdown worms.

Defects in *ife-1* worms include temperature-sensitive secondary spermatocyte arrest, reduced oocyte production and viability, and embryonic arrest (Henderson et al., 2009). Such phenotypes suggest that IFE-1 recruits a defined subpopulation of mRNAs. Our TSAA identified 77 mRNAs that specifically require IFE-1 for efficient translation. The mRNAs encode GTPases (*ran-1*, *rab-5* and *rab-7*) involved in cell signaling pathways required for mitotic spindle formation or vesicle trafficking, Ephrin receptor tyrosine kinase activity (*vab-1* and *vpr-1*) that regulates oocyte maturation, and transcription/splicing factors (*rnp-3*, *let-49* and *lin-26*) necessary for embryonic gene expression (Fig. 1D).

Our data suggest that IFE-1 promotes VAB-1 synthesis in non-maturing oocytes. This Ephrin receptor suppresses the MAPK signaling required for oocytes meiotic maturation (Miller et al., 2003). IFE-1 recruits not only *vab*-1 mRNA, but also those encoding several VAB-1 regulators. These include VPR-1, the VAP ortholog containing an MSP domain that binds VAB-1 *in vitro*; RAN-1, a Ran GTPase that promotes trafficking of VAB-1 to suppress MAPK activity; and RAB-7, a Rab GTPase predicted to traffic VAB-1 to lysosomes (Cheng et al., 2008). Thus, one eIF4E isoform acts through cap-dependent positive mRNA translational control to induce both positive and negative signaling for oocyte maturation (Fig. 7). Additionally, the patterns of MAPK activation showed that IFE-1 suppresses MAPK in young post-pachytene oocytes (prior to the −5 position) independently of VAB-1, suppresses MAPK in proximal (−5 to −1) oocytes through VAB-1, and plays an opposite role in promoting sperm-induced MAPK activation in the mature (−1) oocyte.

We propose that IFE-1 mediates the recruitment of several well-characterized translationally regulated mRNAs in late stage oocytes (e.g. *vab-1*, *rab-7*, *oma-1*, *mex-1* and *pos-1*) (Henderson et al., 2009). Other mRNAs identified in our TSAA screen, and verified by

Journal of Cell Science (2015) 128, 4487-4498 doi:10.1242/jcs.172684

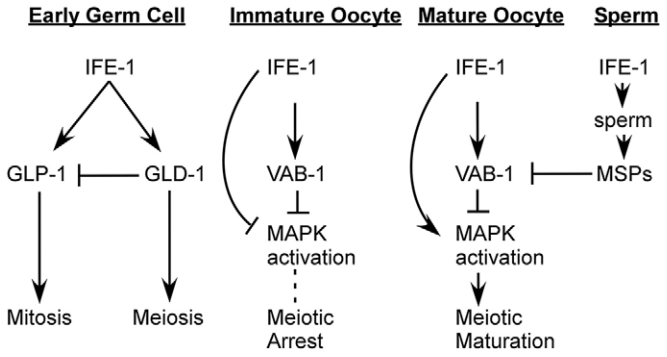

Fig. 7. Working model for the role of IFE-1 in early germ cell meiosis, MAPK suppression or activation, and maturation. The data supports a role for IFE-1 in suppressing MAPK activation in immature oocytes by promoting *vab-1* mRNA translation. In the maturing oocyte, most directly influenced by MSP signaling, IFE-1 has an opposing role in the maturing (−1) oocyte by promoting MAPK activation through other substrates. Finally, IFE-1 also promotes viable sperm MSP production and subsequent MAPK signaling in the maturing oocyte.

polysome resolution of endogenous mRNAs, are also interesting in light of *ife-1* phenotypes. *rnp-3* mRNA, for example, encodes an snRNP-associated spliceosomal protein RNP-3 (also known as U2B) required for embryonic viability. Although redundantly active with RNP-2 (also known as U1A), knockout of *rnp-3* induces embryonic lethality (Saldi et al., 2007). The inability of *ife-1* worms to efficiently translate *rnp-3* mRNA might contribute to the embryonic arrest and reduced fecundity (Amiri et al., 2001). These data indicate that IFE-1 has a substantially broader translational 'reach' than many characterized RNA-binding proteins. IFE-1 induces the selective synthesis of proteins that both promote and suppress cell differentiation, depending upon where and when IFE-1 encounters their mRNAs.

The preferential recruitment of an mRNA by one IFE isoform over another is not likely due to its sequence specificity. eIF4Es bind just the 5′-cap and first two nucleotides of an mRNA (Marcotrigiano et al., 1997). Even though IFE isoforms show individual preferences for either monomethylated or trimethylguanosine caps (Miyoshi et al., 2002), this level of discrimination is still insufficient to explain the mRNA selectivity we have now confirmed for IFE-1, IFE-2 and IFE-4 (Dinkova et al., 2005; Henderson et al., 2009; Song et al., 2010 and this study). Instead, preferential mRNA recruitment might come from interactions of eIF4Es with various 4EBPs (Igreja et al., 2014). The *Drosophila* Mextli protein is one such 4EBP that acts positively to recruit germ cell mRNAs into productive initiation complexes with eIF4E (Hernandez et al., 2013). Of the *C. elegans* eIF4E isoforms, IFE-1 uniquely associates with a 4EBP in P granules known as PGL-1 (Amiri et al., 2001). Notably, our gradient fractionation showed that P granules do not co-sediment or associate with ribosome-bound mRNAs suggesting that P granule mRNAs, which are repressed, must be 'handed off' to translation complexes. Protein–protein complexes involving other eIF4Es and other 4EBPs have been shown to recognize motifs in mRNA 3′UTRs and repress the translation of the bound message (Piqué et al., 2008; Stebbins-Boaz et al., 1999). As bound mRNAs become required, 3′UTR complexes become remodeled such that eIF4E can associate with eIF4G and recruit the message to ribosomes (Cao and Richter, 2002). In *C. elegans*, the *gld-1* mRNA is bound and translationally repressed by a Pumilio homolog (FBF) in the mitotic region of the germ line (Marin et al., 2003). When germ cells migrate away from the niche, *gld-1* mRNA becomes de-repressed and subsequently recruited for translation by IFE-1. As germ cells approach the meiotic region, newly synthesized GLD-1 protein represses the translation of *glp-1* mRNA through 3′UTR interactions. The repression of *glp-1* is an important event in the transition from mitosis to meiosis (Hansen et al., 2004a). We have shown that IFE-1 plays a direct role in both processes by recruiting each mRNA temporally in turn, as demonstrated by biochemical polysome analyses here and in our previous study (Henderson et al., 2009). The *glp-1* and *gld-1* mRNAs both require IFE-1 for their most efficient translation, but the exact role that IFE-1 plays in the transition from mitosis to meiosis remains unclear.

Biochemical polysome fractionation allowed us to directly assay the efficiency of individual mRNAs, but it provided no information on where or when each mRNA was being recruited by IFE-1. Instead, use of a histone H2B–GFP 3′UTR reporter assay permitted us to observe translational control events *in situ* and *in vivo*. We monitored spatiotemporal translational activation of each reporter mRNA within individual living worm gonads with single-cell resolution. Our data suggest that IFE-1 acts early in the shift from mitosis to meiosis by regional translation of *gld-1* mRNA. Additionally, *pos-1* mRNA became de-repressed in late stage oocytes, and this too was dependent on IFE-1. Similar late stage oocyte synthesis of MEX-1 protein in the −3, −2 and −1 oocytes was previously observed to be IFE-1 dependent (Henderson et al., 2009). Both observations suggest that other eIF4E isoforms are not sufficient to recruit either *pos-1* or *mex-1* mRNAs to ribosomes. Not all oocyte mRNAs require IFE-1, as evidenced by unaltered expression of the *tbb-2* control. Interestingly, *pgl-1* mRNA actually translated better in the absence of IFE-1, and its mRNA increased in abundance. This suggests that IFE-1 competes with the other IFEs (e.g. for initiation complexes or free ribosomes) that mediate PGL-1 synthesis. Thus far we can define three classes of germline mRNAs relative to eIF4E isoform IFE-1: those that uniquely require this isoform following de-repression, those that do not require the IFE-1 isoform at all, and those that use other IFEs to greater advantage. Collectively these data suggest that IFE-1 selectively activates mRNAs at the transition from mitosis to meiosis in the distal gonad (*gld-1* and *glp-1*), at MAPK-induced meiotic maturation in the proximal gonad (*vab-1*, *vpr-1*, *rab-7*, *ran-1* and *oma-1*), and in preparation for embryogenesis (*pos-1* and *mex-1*; Fig. 7). As such, IFE-1 guides unique protein synthetic events that punctuate germ cell development throughout gametogenesis for both the sperm and egg.

MATERIALS AND METHODS

Strains

The *C. elegans* strains used were Bristol, N2 wild-type strain, *Caenorhabditis* Genetics Center (CGC) strains AZ212 *unc-119*(ed3), ruls32 [P*pie-1*:GFP:H2B:*tbb-2* 3′UTR +*unc-119*(+)],CZ337 *vab-1* (dx31) II, DH245 *fem-2* (b245) III, JH2060 *unc-119*(ed3) III; axls 1498 [P*pie-1*:GFP:*gld-1* ORF:*gld-1* 3′UTR +*unc-119*(+)], JH2320 *unc-119*(ed3) III; axls 1677 [P*pie-1*:GFP:H2B:*pgl-1* 3′UTR +*unc-119*(+)], JH2427 *unc-119*(ed3) III; axls 1751 [P*pie-1*:GFP:H2B:*pos-1* 3′UTR +*unc-119*(+)]. SS712 [*ife-1*(bn-127)] was obtained from Dr Susan Strome (Molecular, Cell and Developmental Biology, University of California, Santa Cruz). All strains were maintained on normal growth medium (NGM) plates with *E. coli* strain OP50. For sucrose gradient fractionation and polysomal analysis, worms were grown on chicken egg yolk OP50 plates at 20°C. As previously described, mix-staged worm populations were isolated in M9 buffer, sucrose floated and pelleted in liquid nitrogen in the presence of RNase inhibitors (Dinkova et al., 2005).

Microscopy and immunostaining

Worm gonads were prepared for microscopy as previously described (Henderson et al., 2009), with the following exceptions: dissected gonads were fixed in formaldehyde (3% formaldehyde, 1× PBS) for 30 min,

washed with PTW (1× PBS and 0.1% Tween 20), and stored at −20°C in methanol. To prepare gonads for immunostaining, samples were reconstituted and washed with PTW. Gonads were blocked overnight in PTWB (PTW plus 0.5% BSA) at 4°C. The anti-diphospho-MAPK (activated) mouse monoclonal antibody (catalog no. F7776; Sigma) was diluted 1:200 in PTWB and incubated with samples at room temperature for 2 h. Following another PTWB wash, goat anti-mouse-IgG conjugated to Alexa Fluor 488 (Invitrogen) at 1:400 was used as the secondary antibody. Samples were washed in PTWB and mounted on 1.2% agarose pads with 5 µl Vectashield (Vector Laboratories) with DAPI. Gonads were imaged on an Axiovert 200 M inverted microscope (Carl Zeiss) using DIC, FITC, and DAPI filter cubes and analyzers. Images were analyzed with Axiovision 4.3 software (Carl Zeiss).

RNAi feeding conditions

Bacterial transformation and feeding techniques were as described previously (Contreras et al., 2008), with the following exceptions. The *ife-1*-specific plasmid (pT72id) was constructed by subcloning 153 bp (nt 589–741) of *ife-1* cDNA sequence into plasmid pL4440. Double-stranded RNA was expressed in *E. coli* strain HT115(DE3) in culture containing tetracycline and ampicillin and was induced with IPTG. Induced cultures were grown on NGM agar medium plates supplemented with tetracycline, ampicillin and IPTG. Strains were synchronized and L3 or L4 hermaphrodites were transferred onto seeded RNAi plates at 22°C for 36–40 h. Hermaphrodites were transferred to RNAi plates, with a limit of three F0 adults per plate and incubated at 25°C for 24 h. F0 adults were then removed. The F1 generation was incubated at 25°C for another 24 h. Progeny were dissected or directly utilized for microscopy.

Live worm fluorescence imaging and quantification

Adult hermaphrodites were transferred onto agarose pads with Vectashield mounting medium with DAPI for microscopy. AxioVision V4.8.2 (Carl Zeiss) was used to identify optimal exposure time (OET) for linear fluorescence output. Images were acquired along a time gradient of −40% OET, −20% OET, OET, +20% OET and +40% OET. A measurement for regions of interest (ROIs) was defined manually for each image. The densiometric mean was within each ROI and assembled on an Excel spreadsheet. Background fluorescence was defined from the *y*-intercept of the linear regression derived by plotting densiometric mean versus the percentage OET. Mean fluorescence at OET minus background fluorescence was divided by OET. Multiple values of mean fluorescence per exposure time were used to derive average values and standard deviations presented in the graphs in Fig. 4. *P* values were calculated using a two-tailed *t*-test. ROIs were defined for the distal region of immature oocytes (*gld-1* 3′UTR reporter) or for expression in the nucleus of individual oocytes (*tbb-2*, *pos-1* and *pgl-1*).

Sucrose gradient fractionation of polysomes, qPCR and western blotting

Sucrose gradient fractionation (10–45%) was performed on wild-type and *ife-1*(*bn127*) worms as previously described (Dinkova et al., 2005) with modifications (Henderson et al., 2009). Profiles of the gradient were collected by continuous monitoring of the UV absorbance at 254 nm. It should be noted that profiles take on a different character from experiment to experiment, depending upon the amount of worm lysate loaded, the sensitivity of the UV monitor, and the exact centrifugation parameters of a run, as we have seen in previous publications (Dinkova et al., 2005; Henderson et al., 2009). This does not indicate changes in measured translation between experiments (e.g. polysome number), merely different placement (e.g. fraction number of a tetramer polysome or the *gpd-3* control peak). For that reason, direct comparisons are made only between separate worm samples from the same sedimentation run (Fig. 2). For the TSAA (Fig. 1), however, three similar but separate sedimentation runs were used to normalize variability for general comparison.

Sample preparation for qPCR was identical to that previously described (Dinkova et al., 2005), except that RNA from gradient fractions was isolated in four volumes of Trizol (Invitrogen). RNA was isolated from one half of each 1-ml gradient fraction. cDNA was synthesized using Verso cDNA synthesis kit (Thermo Scientific). qPCR was performed on biological duplicates using an Sso Fast Evagreen Super mix (Bio-Rad) in an iCycler iQ5 Real-time PCR machine, following the manufacturer's protocol. Primer sequences used were: *gpd-3* (forward 5′-GATCTCAGCTGGGTCTCTT-3′, reverse 5′-TCCAGTACGATTCCACTCAC-3′); *rnp-3* (forward 5′-CGATCTATGTGAACAATCTCAA-3′, reverse 5′-ACCGAATTGTGTGAAAACC-3′); *rab-7* (forward 5′-GCTCGGAGTCGCTTTTTATC-3′, reverse 5′-GGACAAACGGGAAATGGTCT-3′); *vpr-1* (forward 5′-ACGAGGATAGTTTTGCTTCTT-3′, reverse 5′-ACTGTCGATTTCAACGATTT-3′); *gld-1* (forward 5′-TTCAGGTCCAGTTTTGATGT-3′, reverse 5′-GACGTTAGATCCGAGAAGGT-3′); *vab-1* (forward 5′-AAGAATATTGGACGGTTGG-3′, reverse 5′-GTCGCATATTCGGTAGTAAA-3′); *ran-1* (forward 5′-ACTTGTCTTCCACACCAATC-3′, reverse 5′-GAGCGGTAACATCGAACA-3′). The real-time quantification of each mRNA was normalized to total RNA content. For detection of PGL-1 protein across the gradient, 20 µl of each fraction was mixed directly with an equal volume of SDS loading buffer and subjected to SDS-PAGE on a 10% gel, then immunoblotted with 1:2000 dilution of rabbit anti-PGL-1 antiserum as previously described (Amiri et al., 2001; Kawasaki et al., 1998).

Translational state array analysis

Three independent sets of 10–45% sucrose gradients were prepared for wild-type (denoted by the designator w in equations below) and *ife-1*(*bn127*) worms (denoted by the designator i in equations below) as previously described (Dinkova et al., 2005; Henderson et al., 2009). Following RNA isolation from individual fractions, non-polysomal (NP) fractions 1–4 and polysomal (P) fractions 6–12 were pooled separately. Fraction 5 contained the 80S peak. These twelve samples were purified and hybridized to Affymetrix *C. elegans* arrays (UNC Functional Genomics Core Facility). We created formulas in Excel to compare raw microarray hybridization signal values with ratios that were normalized to total non-polysomal and polysomal mRNA signals. [Pw/(NPw+Pw)]=Rw, [Pi/(NPi+Pi)]=Ri, [Rw/Ri]=relative fold change in R (MFR). Summing the non-polysomal and polysomal signals (NP+P) from single replicates, we also accounted for the mean fold change in total mRNA (MFT, Fig. S4). Affymetrix returned a probe signal output value for each of 22,625 genes. Each gene was tagged as being statistically 'present' or 'absent' for each of the four samples (Pw, NPw, Pi and NPi). Signals flagged as 'absent' by Affymetrix in three or more of the four samples for a single replicate were removed. This analysis was performed in three biological replicates. Any mRNAs that did not pass the present or absent test in all three replicates were removed from the dataset, leaving a representative group of 13,372 mRNAs. The entire microarray dataset has now been submitted to GEO under the accession number GSE74459. To derive mRNAs translationally regulated by IFE-1 only, mRNAs with an MFR greater than 1.5 fold and an MFR−s.d.>1 were considered. This yielded a prioritized list of 77 mRNAs with decreased translational efficiency in the absence of IFE-1. mRNAs were identified by cross-referencing information provided by Affymetrix with WormBase and GeneBank online resources.

Acknowledgements

We thank Drs Kyle Mansfield and Chris Geyer for improving this manuscript. The *fem-2*, *vab-1*, and all of the GFP–3′UTR strains were provided by the *Caenorhabditis* Genetics Center, which is funded by NIH Office of Research Infrastructure Programs [grant number P40 OD010440].

Competing interests

The authors declare no competing or financial interests.

Author contributions

Experiments were conducted by A.J.F. and M.A.H. with help from J.K.M., J.L.H. and B.D.K. The manuscript was written by A.J.F. and B.D.K.

Funding

This work was supported by the National Science Foundation (NSF) [grant number MCB0842475 to B.D.K.].

Supplementary information

Supplementary information available online at
http://jcs.biologists.org/lookup/suppl/doi:10.1242/jcs.172684/-/DC1

References

Amiri, A., Keiper, B. D., Kawasaki, I., Fan, Y., Kohara, Y., Rhoads, R. E. and Strome, S. (2001). An isoform of eIF4E is a component of germ granules and is required for spermatogenesis in C. elegans. *Development* **128**, 3899-3912.

Barnard, D. C., Cao, Q. and Richter, J. D. (2005). Differential phosphorylation controls Maskin association with eukaryotic translation initiation factor 4E and localization on the mitotic apparatus. *Mol. Cell. Biol.* **25**, 7605-7615.

Cao, Q. and Richter, J. D. (2002). Dissolution of the maskin-eIF4E complex by cytoplasmic polyadenylation and poly(A)-binding protein controls cyclin B1 mRNA translation and oocyte maturation. *EMBO J.* **21**, 3852-3862.

Chappell, V. A., Busada, J. T., Keiper, B. D. and Geyer, C. B. (2013). Translational activation of developmental messenger RNAs during neonatal mouse testis development. *Biol. Reprod.* **89**, 61.

Cheng, H., Govindan, J. A. and Greenstein, D. (2008). Regulated trafficking of the MSP/Eph receptor during oocyte meiotic maturation in C. elegans. *Curr. Biol.* **18**, 705-714.

Contreras, V., Richardson, M. A., Hao, E. and Keiper, B. D. (2008). Depletion of the cap-associated isoform of translation factor eIF4G induces germline apoptosis in C. elegans. *Cell Death Differ.* **15**, 1232-1242.

De Benedetti, A. and Graff, J. R. (2004). eIF-4E expression and its role in malignancies and metastases. *Oncogene* **23**, 3189-3199.

De Benedetti, A. and Rhoads, R. E. (1990). Overexpression of eukaryotic protein synthesis initiation factor 4E in HeLa cells results in aberrant growth and morphology. *Proc. Natl. Acad. Sci. USA* **87**, 8212-8216.

Detwiler, M. R., Reuben, M., Li, X., Rogers, E. and Lin, R. (2001). Two zinc finger proteins, OMA-1 and OMA-2, are redundantly required for oocyte maturation in C. elegans. *Dev. Cell* **1**, 187-199.

Dinkova, T. D., Keiper, B. D., Korneeva, N. L., Aamodt, E. J. and Rhoads, R. E. (2005). Translation of a small subset of Caenorhabditis elegans mRNAs is dependent on a specific eukaryotic translation initiation factor 4E isoform. *Mol. Cell. Biol.* **25**, 100-113.

Dworkin, M. B. and Dworkin-Rastl, E. (1990). Functions of maternal mRNA in early development. *Mol. Reprod. Dev.* **26**, 261-297.

Francis, R., Barton, M. K., Kimble, J. and Schedl, T. (1995). gld-1, a tumor suppressor gene required for oocyte development in Caenorhabditis elegans. *Genetics* **139**, 579-606.

Friday, A. J. and Keiper, B. D. (2015). Positive mRNA translational control in germ cells by initiation factor selectivity. *Biomed. Res. Int.* **2015**, 327963.

Fukuyo, A., In, Y., Ishida, T. and Tomoo, K. (2011). Structural scaffold for eIF4E binding selectivity of 4E-BP isoforms: crystal structure of eIF4E binding region of 4E-BP2 and its comparison with that of 4E-BP1. *J. Pept. Sci.* **17**, 650-657.

Furic, L., Rong, L., Larsson, O., Koumakpayi, I. H., Yoshida, K., Brueschke, A., Petroulakis, E., Robichaud, N., Pollak, M., Gaboury, L. A. et al. (2010). eIF4E phosphorylation promotes tumorigenesis and is associated with prostate cancer progression. *Proc. Natl. Acad. Sci. USA* **107**, 14134-14139.

Ghosh, S. and Lasko, P. (2015). Loss-of-function analysis reveals distinct requirements of the translation initiation factors eIF4E, eIF4E-3, eIF4G and eIF4G2 in Drosophila spermatogenesis. *PLoS ONE* **10**, e0122519.

Gingras, A.-C., Raught, B. and Sonenberg, N. (1999). eIF4 initiation factors: effectors of mRNA recruitment to ribosomes and regulators of translation. *Annu. Rev. Biochem.* **68**, 913-963.

Goodwin, E. B. and Evans, T. C. (1997). Translational control of development in C. elegans. *Semin. Cell Dev. Biol.* **8**, 551-559.

Graff, J. R., Konicek, B. W., Carter, J. H. and Marcusson, E. G. (2008). Targeting the eukaryotic translation initiation factor 4E for cancer therapy. *Cancer Res.* **68**, 631-634.

Hansen, D., Albert Hubbard, E. J. and Schedl, T. (2004a). Multi-pathway control of the proliferation versus meiotic development decision in the Caenorhabditis elegans germline. *Dev. Biol.* **268**, 342-357.

Hansen, D., Wilson-Berry, L., Dang, T. and Schedl, T. (2004b). Control of the proliferation versus meiotic development decision in the C. elegans germline through regulation of GLD-1 protein accumulation. *Development* **131**, 93-104.

Henderson, M. A., Cronland, E., Dunkelbarger, S., Contreras, V., Strome, S. and Keiper, B. D. (2009). A germline-specific isoform of eIF4E (IFE-1) is required for efficient translation of stored mRNAs and maturation of both oocytes and sperm. *J. Cell Sci.* **122**, 1529-1539.

Hernandez, G., Miron, M., Han, H., Liu, N., Magescas, J., Tettweiler, G., Frank, F., Siddiqui, N., Sonenberg, N. and Lasko, P. (2013). Mextli is a novel eukaryotic translation initiation factor 4E-binding protein that promotes translation in Drosophila melanogaster. *Mol. Cell. Biol.* **33**, 2854-2864.

Hodgkin, J. (1986). Sex determination in the nematode C. elegans: analysis of tra-3 suppressors and characterization of fem genes. *Genetics* **114**, 15-52.

Hunt, P. A. (1998). The control of mammalian female meiosis: factors that influence chromosome segregation. *J. Assist. Reprod. Genet.* **15**, 246-252.

Igreja, C., Peter, D., Weiler, C. and Izaurralde, E. (2014). 4E-BPs require non-canonical 4E-binding motifs and a lateral surface of eIF4E to repress translation. *Nat. Commun.* **5**, 4790.

Jankowska-Anyszka, M., Lamphear, B. J., Aamodt, E. J., Harrington, T., Darzynkiewicz, E., Stolarski, R. and Rhoads, R. E. (1998). Multiple isoforms of eukaryotic protein synthesis initiation factor 4E in Caenorhabditis elegans can distinguish between mono- and trimethylated mRNA cap structures. *J. Biol. Chem.* **273**, 10538-10542.

Jeong, J., Verheyden, J. M. and Kimble, J. (2011). Cyclin E and Cdk2 control GLD-1, the mitosis/meiosis decision, and germline stem cells in Caenorhabditis elegans. *PLoS Genet.* **7**, e1001348.

Jones, A. R., Francis, R. and Schedl, T. (1996). GLD-1, a cytoplasmic protein essential for oocyte differentiation, shows stage- and sex-specific expression during Caenorhabditis elegans germline development. *Dev. Biol.* **180**, 165-183.

Kawasaki, I., Shim, Y.-H., Kirchner, J., Kaminker, J., Wood, W. B. and Strome, S. (1998). PGL-1, a predicted RNA-binding component of germ granules, is essential for fertility in C. elegans. *Cell* **94**, 635-645.

Kawasaki, I., Jeong, M.-H. and Shim, Y.-H. (2011). Regulation of sperm-specific proteins by IFE-1, a germline-specific homolog of eIF4E, in C. elegans. *Mol. Cells* **31**, 191-197.

Keiper, B. D., Lamphear, B. J., Deshpande, A. M., Jankowska-Anyszka, M., Aamodt, E. J., Blumenthal, T. and Rhoads, R. E. (2000). Functional characterization of five eIF4E isoforms in Caenorhabditis elegans. *J. Biol. Chem.* **275**, 10590-10596.

Kelly, W. G. and Fire, A. (1998). Chromatin silencing and the maintenance of a functional germline in Caenorhabditis elegans. *Development* **125**, 2451-2456.

Kimble, J. and Crittenden, S. (2007). Control of germline stem cells, entry into meiosis, and the sperm/oocyte decision in Caenorhabditis elegans. *Annu. Rev. Cell Dev. Biol.* **23**, 405-433.

Ko, S. Y., Guo, H., Barengo, N. and Naora, H. (2009). Inhibition of ovarian cancer growth by a tumor-targeting peptide that binds eukaryotic translation initiation factor 4E. *Clin. Cancer Res.* **15**, 4336-4347.

Kouvaraki, M. A., Liakou, C., Paraschi, A., Dimas, K., Patsouris, E., Tseleni-Balafouta, S., Rassidakis, G. Z. and Moraitis, D. (2011). Activation of mTOR signaling in medullary and aggressive papillary thyroid carcinomas. *Surgery* **150**, 1258-1265.

Lamphear, B. J., Kirchweger, R., Skern, T. and Rhoads, R. E. (1995). Mapping of functional domains in eukaryotic protein synthesis initiation factor 4G (eIF4G) with picornaviral proteases: implications for cap-dependent and cap-independent translational initiation. *J. Biol. Chem.* **270**, 21975-21983.

Lee, M. H., Mamillapalli, S. S., Keiper, B. D. and Cha, D. S. (2015). A systematic mRNA control mechanism for germline stem cell homeostasis and cell fate specification. *BMB Rep.* **2015**, 3259.

Liu, Y., Kuersten, S., Huang, T., Larsen, A., MacMorris, M. and Blumenthal, T. (2003). An uncapped RNA suggests a model for Caenorhabditis elegans polycistronic pre-mRNA processing. *RNA* **9**, 677-687.

Lu, C., Srayko, M. and Mains, P. E. (2004). The Caenorhabditis elegans microtubule-severing complex MEI-1/MEI-2 katanin interacts differently with two superficially redundant beta-tubulin isotypes. *Mol. Biol. Cell* **15**, 142-150.

Macdonald, P. M. and Smibert, C. A. (1996). Translational regulation of maternal mRNAs. *Curr. Opin. Genet. Dev.* **6**, 403-407.

Marcotrigiano, J., Gingras, A.-C., Sonenberg, N. and Burley, S. K. (1997). Cocrystal structure of the messenger RNA 5′ cap-binding protein (eIF4E) bound to 7-methyl-GDP. *Cell* **89**, 951-961.

Marin, V. A., Evans, T. C., Barbee, S. A. and Lublin, A. L. (2003). Translational repression of a C. elegans Notch mRNA by the STAR/KH domain protein GLD-1. *Development* **130**, 2623-2632.

McCarter, J., Bartlett, B., Dang, T. and Schedl, T. (1999). On the control of oocyte meiotic maturation and ovulation in Caenorhabditis elegans. *Dev. Biol.* **205**, 111-128.

Mendez, R. and Richter, J. D. (2001). Translational control by CPEB: a means to the end. *Nat. Rev. Mol. Cell Biol.* **2**, 521-529.

Merritt, C., Rasoloson, D., Ko, D. and Seydoux, G. (2008). 3′ UTRs are the primary regulators of gene expression in the C. elegans germline. *Curr. Biol.* **18**, 1476-1482.

Miller, M. A., Ruest, P. J., Kosinski, M., Hanks, S. K. and Greenstein, D. (2003). An Eph receptor sperm-sensing control mechanism for oocyte meiotic maturation in Caenorhabditis elegans. *Genes Dev.* **17**, 187-200.

Miyoshi, H., Dwyer, D. S., Keiper, B. D., Jankowska-Anyszka, M., Darzynkiewicz, E. and Rhoads, R. E. (2002). Discrimination between mono- and trimethylated cap structures by two isoforms of Caenorhabditis elegans eIF4E. *EMBO J.* **21**, 4680-4690.

Nousch, M. and Eckmann, C. R. (2013). Translational control in the Caenorhabditis elegans germ line. *Adv. Exp. Med. Biol.* **757**, 205-247.

Parisi, M. and Lin, H. (2000). Translational repression: a duet of Nanos and Pumilio. *Curr. Biol.* **10**, R81-R83.

Piqué, M., López, J. M., Foissac, S., Guigó, R. and Méndez, R. (2008). A combinatorial code for CPE-mediated translational control. *Cell* **132**, 434-448.

Rosenwald, I. B. (2004). The role of translation in neoplastic transformation from a pathologist's point of view. *Oncogene* **23**, 3230-3247.

Rosenwald, I. B., Lazaris-Karatzas, A., Sonenberg, N. and Schmidt, E. V. (1993). Elevated levels of cyclin D1 protein in response to increased expression of eukaryotic initiation factor 4E. *Mol. Cell. Biol.* **13**, 7358-7363.

Saldi, T., Wilusz, C., MacMorris, M. and Blumenthal, T. (2007). Functional redundancy of worm spliceosomal proteins U1A and U2B″. *Proc. Natl. Acad. Sci. USA* **104**, 9753-9757.

Salehi, Z. and Mashayekhi, F. (2006). Expression of the eukaryotic translation initiation factor 4E (eIF4E) and 4E-BP1 in esophageal cancer. *Clin. Biochem.* **39**, 404-409.
Schisa, J. A., Pitt, J. N. and Priess, J. R. (2001). Analysis of RNA associated with P granules in germ cells of C. elegans adults. *Development* **128**, 1287-1298.
Seydoux, G., Mello, C. C., Pettitt, J., Wood, W. B., Priess, J. R. and Fire, A. (1996). Repression of gene expression in the embryonic germ lineage of C. elegans. *Nature* **382**, 713-716.
Song, Y. and Lu, B. (2011). Regulation of cell growth by Notch signaling and its differential requirement in normal vs. tumor-forming stem cells in Drosophila. *Genes Dev.* **25**, 2644-2658.
Song, A., Labella, S., Korneeva, N. L., Keiper, B. D., Aamodt, E. J., Zetka, M. and Rhoads, R. E. (2010). A C. elegans eIF4E-family member upregulates translation at elevated temperatures of mRNAs encoding MSH-5 and other meiotic crossover proteins. *J. Cell Sci.* **123**, 2228-2237.
Stebbins-Boaz, B., Cao, Q., de Moor, C. H., Mendez, R. and Richter, J. D. (1999). Maskin is a CPEB-associated factor that transiently interacts with eIF-4E. *Mol. Cell* **4**, 1017-1027.
Syntichaki, P., Troulinaki, K. and Tavernarakis, N. (2007). eIF4E function in somatic cells modulates ageing in Caenorhabditis elegans. *Nature* **445**, 922-926.
Truitt, M. L., Conn, C. S., Shi, Z., Pang, X., Tokuyasu, T., Coady, A. M., Seo, Y., Barna, M. and Ruggero, D. (2015). Differential requirements for eIF4E dose in normal development and cancer. *Cell* **162**, 59-71.
Wormington, M. (1993). Poly(A) and translation: development control. *Curr. Opin. Cell Biol.* **5**, 950-954.